



## Research

**Cite this article:** Borodich FM, Pepelyshev A. 2024 Synthesis of engineering surfaces using representative elementary patterns of roughness. *Proc. R. Soc. A* **480**: 20240242. <https://doi.org/10.1098/rspa.2024.0242>

Received: 8 April 2024

Accepted: 24 July 2024

**Subject Category:**

Engineering

**Subject Areas:**

mechanical engineering, statistics

**Keywords:**

roughness, statistics, moving window, time-series analysis

**Author for correspondence:**

Andrey Pepelyshev

e-mail: [pepelyshevan@cardiff.ac.uk](mailto:pepelyshevan@cardiff.ac.uk)

Electronic supplementary material is available online at <https://doi.org/10.6084/m9.figshare.c.7441730>.

# Synthesis of engineering surfaces using representative elementary patterns of roughness

Feodor M. Borodich<sup>1</sup> and Andrey Pepelyshev<sup>2</sup>

<sup>1</sup>College of Aerospace Engineering, Chongqing University, Chongqing, People's Republic of China

<sup>2</sup>School of Mathematics, Cardiff University, Senghennydd Road, Cardiff CF24 4AG, UK

AP, 0000-0001-5634-5559

Synthesis of surface roughness is a long-standing problem that has many practical applications. Here novel algorithms for the synthesis of rough surfaces at nano/micro scales are proposed. The algorithms are based on introduction and development of two new concepts, namely the representative elementary pattern of roughness (REPR) and the statistically representative pattern of surface roughness (SRPSR). From the statistical point of view, the REPR is the smallest interval (or area) over which a measurement can be made that represents statistically the whole surface. However, synthesis of surfaces by the direct use of the REPR may cause some artificial singularities. To avoid this drawback and to incorporate the synthetic surface in a numerical scheme of the contact solver, one needs to extend the REPR to a non-singular SRPSR that satisfies additional conditions of the scheme used. Our findings indicate that specific time-series analysis techniques, such as the moving window approach, can be effectively utilized to extract the REPR from experimental data. The representativeness may be justified by the use of the Kolmogorov–Smirnov statistic. Extraction of REPRs of surfaces and constructions of appropriate SRPSRs are demonstrated on experimental data obtained by stylus and atomic-force microscopy at micro and atomic/nano scales, respectively.

## 1. Introduction

Measurements of the surface topography and analysis of roughness have been intensively studied for decades (e.g. [1]). Indeed, friction, wear and energy dissipation during interacting of engineering surfaces are strongly influenced by asperity deformations and these are controlled by the surface topography. Across various preparation methods, a defining characteristic of most engineering surfaces is the inherent presence of finite-scale roughness (e.g. [2–4]). Surface roughness is a critical parameter influencing component performance across numerous industries, particularly in precision engineering applications. Surface roughness becomes particularly essential for understanding dry friction mechanisms in the absence of liquid lubricants, such as in nano/micro-scale devices and those operating in vacuum environments.

Nowadays there exist various solvers for numerical simulations of contact between rough solids, e.g. the Polonsky–Keer method [5,6]. Formally, one could use directly the real experimental roughness data in a contact solver. Advanced experimental techniques, exemplified by Atomic Force Microscopy (AFM), enable researchers to characterize surface topography with atomic-scale resolution [7]. However, this would not allow the researchers to simulate many tribological phenomena. The difficulty may be described by the Lubrecht–Venner statement: though calculating a tribological problem for a single, real rough surface might be theoretically possible, its limited generalizability to other rough surfaces or even slight variations in the same surface renders it impractical [8]. Indeed, for such a prediction, one needs to have a warranty that the rough surface used in the contact solver is entirely typical of the whole surface on average at scales that are governing for the tribological process under consideration.

Surface synthesis statistically replicates the topographical characteristics of a real surface by creating a synthetic counterpart that mimics its statistical properties. Thus, synthesis of roughness is the crucial process for numerical and analytical simulations of contact between rough surfaces and other problems of tribology including friction and wear because the synthetic surfaces may be incorporated into numerical solvers of contact between rough surfaces.

Evaluation of statistical characteristics of surface roughness and synthesis of rough surfaces are longstanding research topics (e.g. [9,10]). Although synthesis of rough surfaces is widely used in various industries, the current statistical approaches to description of surface roughness are rather primitive. Indeed, despite the plethora of over 30 statistical roughness parameters in use, a clear understanding of how roughness influences dry contact and friction remains elusive [11]. Note that synthetic surfaces that model only some surface characteristics do not give a warranty that the rough surface used in the contact solver is entirely typical of the whole surface on average for the tribological process under consideration.

Consider a two-dimensional/three-dimensional roughness profile with a large number of points, which is obtained by some technical device, e.g. by a profilometer or AFM. Let us study a problem of synthesis of another shorter two-dimensional/three-dimensional profile that has the same height distribution as the large profile. Doing this, we may think that the large profile is obtained by a replication of some pattern given by the shorter profile. Two new concepts are introduced here: (i) the representative elementary pattern of roughness (REPR) and (ii) the statistically representative pattern of surface roughness (SRPSR). From the statistical point of view, the REPR is the smallest interval (or area) over which a measurement can be made that will yield a value representative of the whole surface, while the SRPSR not only ensures statistical representativeness of the entire surface but also adheres to additional criteria based on the specific contact problem and numerical approach. It is proposed in this paper to modify some techniques of time-series analysis (e.g. [12]) and apply them to roughness of engineering surfaces. It is known that the Kolmogorov–Smirnov (KS) statistic may test whether the empirical distribution of data is different than a reference distribution. It is shown that the combination of the moving window technique and the KS statistic effectively extracted the REPR of the surfaces. Hence, simpler surfaces with equivalent roughness in terms of the height

distribution may be synthesized. Contrary to the most current statistical approaches to surface roughness description, there is no need to assume the Gaussian distribution of heights or fractal character of roughness at the micro or atomic/nano scales.

## 2. Preliminaries: synthesis of tribological surfaces

### (a) The Fourier and wavelet approaches to synthesis of surfaces

Surface analysis often utilizes Fourier decomposition, breaking down the measurement data into a series of sine and cosine functions. In Fourier analysis of surfaces, the first harmonic reveals deviations of the measured profile from the nominal shape at a specific scale. If so, then this is attributed to surface waviness, while roughness may be considered as the noise of the surface shape. Thus, in surface topography, long wavelength features are termed ‘waviness’, while short wavelength irregularities are classified as ‘roughness’. It is often argued [1] that surface waviness should be measured apart from its roughness.

We will consider further only nominally flat surfaces. The intersection between a plane perpendicular to a surface and the surface itself is called the surface profile. The rough profile may be presented as graph of a function  $z(x)$ ,  $x \in [-L, L]$ . Let  $\bar{z}$  denote the mean profile line, i.e.

$\bar{z} = \frac{1}{2L} \int_{-L}^L z(x) dx$  is the average value of the profile function  $z(x)$ . If the origin level of the height measurements is taken at  $\bar{z}$  then

$$\frac{1}{2L} \int_{-L}^L [z(x) - \bar{z}] dx = 0.$$

The measurement data may be decomposed by the use of other orthogonal non-trigonometric functions. Usually such functions having compact supports are called wavelets, and a decomposition of measurement data using such functions is called wavelet transform. Although there are several distinctions between the Fourier and wavelet approaches, the main idea of the wavelet transform is the same. One can use Fourier or wavelet synthesis when the synthetic surface is represented as the sum of the measurement decomposition using the bounded number of the basis functions (e.g. [3,10]). Both kinds of surface synthesis do not provide a warranty that the surface obtained represents the original one and the Lubrecht–Venner statement (formulated in §1) is applicable to synthesized surfaces [8].

### (b) Characterization of nominally flat surfaces

Characterization of nominally flat surfaces may be roughly split into two partially overlapping approaches: (i) selection of several roughness parameters and (ii) modelling of surface topography as a realization of a random process.

#### (i) Surface description based on selected parameters of roughness

Apparently, Abbott & Firestone [13] pioneered the application of statistical tools to analyse surface roughness. They suggested to calculate the right-tailed cumulative distribution function of the surface heights  $\Phi(z)$ . If one considers the probability density function  $\phi(z)$  that shows the probability that the height  $z(x)$  at a surface point  $x$  is between  $z$  and  $z + dz$ , then  $\Phi(z)$  is defined as

$$\Phi(z) = \int_z^{\infty} \phi(t) dt. \quad (2.1)$$

Tribology utilizes the Abbott–Firestone curve, also known as the bearing area curve, to potentially correlate it with the contact properties of rough surfaces. Its value at a level  $z = h$  is equal to the normalized length (the area in the two-dimensional problem) of the slice of the profile above the level  $h$ . In some cases, this curve can be leveraged to estimate the force exerted during the penetration of a rough solid into an elastic foundation. Indeed, for a thin elastic layer contacting a punch with a large contact area compared with the layer's thickness, the leading term of the asymptotic solution can be approximated by the Fuss–Winkler foundation model (refer, e.g. to a review by Borodich *et al.* [14] and references therein).

Zhuravlev [15] used the probability density function  $\phi(z)$  and represented rough surfaces as a collection of spherical protuberances having identical radii but located at different heights. Then he developed his statistical model of contact between rough solids. A similar model was developed by Greenwood & Williamson [16]. Zhuravlev–Greenwood–Williamson-type models require knowledge of the summit radii of surface asperities. If the roughness is isotropic then the surface roughness  $z(x, y)$  is characterized by just a profile  $z(x)$ . If the profile heights  $z_k = z(x_k)$  are measured with a regular stylus or AFM step  $\tau$ , i.e. one has  $x_k = x_0 + k\tau$ , then the curvature ( $\kappa$ ) of a protuberance  $z_k$  can be defined as

$$\kappa = -(z_{k-1} + z_{k+1} - 2z_k)/\tau^2,$$

where  $z_{k-1} < z_k$  and  $z_{k+1} < z_k$ , refer to [3]. Whitehouse & Archard [17] demonstrated that the mean curvature of a rough surface is scale-dependent, varying with the chosen sampling interval.

The introduction of the Abbott–Firestone curve provoked a period of intense research, characterized by the generation of numerous statistical roughness parameters, called the ‘parameter rash’ [18]. The characterization encompassed both the vertical height distribution and the horizontal profile distribution of the roughness. Apparently the most popular height parameter is the maximum height  $R_{\max}$  of the profile  $z(x)$  defined on an interval  $[-L, L]$  such that  $\bar{z} = 0$ , that is defined as

$$R_{\max} = \max_{x \in [-L, L]} z(x).$$

The arithmetical mean deviation of the surface  $R_a$  and the root mean square height  $R_q$  or  $\sigma^2$  are also very popular parameters of surface roughness

$$R_a = \frac{1}{2L} \int_{-L}^L |z(x)| dx \approx \frac{\sum_{i=1}^n |z(x_i)|}{n}, \quad R_q = \sigma = \left[ \frac{1}{2L} \int_{-L}^L [z(x)]^2 dx \right]^{1/2}, \quad (2.2)$$

where  $n$  is the number of points of measurements on the interval and  $z(x_i)$  is the measured height at the point  $x_i$ . Note that  $R_q$  is the square root of the mean square deviation with respect to the mean profile line  $\bar{z} = 0$ .

While certain statistical roughness parameters hold value in specific engineering applications, many lack general applicability [18]. In fact, engineers have to describe the rough surfaces using just a few roughness parameters. It is not clear what parameters they have to use for a particular tribological process under consideration because the European and British standard [19] contains over 20 surface and profile parameters, while the American Standard [20] is also a very long document that includes all parameters of the European Standard and many additional parameters. In particular, it contains ‘Section 10 – Terminology and Procedures for Evaluation of Surface Textures Using Fractal Geometry’. Despite claims of fractal dimension being a scale-independent roughness parameter, its fractal behaviour typically holds only over a limited range of about 1.5 orders of magnitude [10,21]. As has been mentioned, there are many other parameters of surface roughness and it is practically impossible to include all of them in synthetic surfaces. In general, the complex contact mechanics of rough surfaces defy description using a finite set of parameters.

## (ii) Surface topography as a realization of a stochastic process

Linnik & Khusu [22,23] suggested to model rough surfaces as realizations of Gaussian (normal) processes. Whitehouse & Archard [17] introduced independently a similar approach and they noted correctly that a Gaussian surface is completely defined by two parameters, a height mean  $\bar{z}$  and an auto-covariance function  $R(\delta)$

$$R(\delta) = \lim_{T \rightarrow \infty} \frac{1}{2T} \int_{-T}^T [z(x + \delta) - \bar{z}][z(x) - \bar{z}] dx = \langle [z(x + \delta) - \bar{z}][z(x) - \bar{z}] \rangle.$$

The function  $R(\delta)$  characterizes the horizontal distribution of asperities of a rough surface profile. Indeed, Maugis [24] emphasized the need to consider both vertical and horizontal roughness distributions, as surfaces can share height and peak height characteristics yet differ in horizontal extension. Instead of  $R(\delta)$ , one can use its Fourier transform, the power spectral density (PSD)  $G(\omega)$  of the signal frequency  $\omega$

$$G(\omega) = \frac{2}{\pi} \int_0^{\infty} R(\delta) \cos \omega \delta d\delta \quad \text{and} \quad \bar{z} = \lim_{T \rightarrow \infty} \frac{1}{2T} \int_{-T}^T z(x) dx.$$

Gaussian surfaces were later intensively studied (e.g. [2,3,24–26]). Stochastic processes with non-Gaussian height distributions can be constructed using an approach described in [27].

There exist various tests of normality of experimental data [28]. These include the KS, Lilliefors, Shapiro–Wilk, Anderson–Darling, Cramer–von Mises, Pearson and Shapiro–Francia normality tests. Applications of these tests to typical experimental data showed that (i) the height distribution is not normal either at nanometre or microscale for rough metallic surfaces prepared by grinding [29], (ii) the height distribution is normal for polishing papers of different nominal asperity sizes [30] and (iii) AFM measurements at 117 nm steps revealed normality of microscale and nanoscale roughness for carbon coatings deposited by DC-pulsed magnetron sputtering, while 10 nm steps identified a departure from normality in the roughness of the non-biased sample [31]. Thus, the prevalence of non-Gaussian characteristics in real-world surfaces necessitates the exploration of alternative models beyond those designed for Gaussian landscapes.

## (iii) Fractal and PSD approaches to surface roughness

Many different surface topographies were studied by Sayles & Thomas [32]. They obtained an experimental relation between normalized PSD and wavelength. Logarithmic plotting yielded a remarkably consistent trend across a vast range, spanning micrometres to metres. Berry & Hannay [33] argued that these results are a particular case of fractal surfaces. However, the PSD approach has not a lot of sense if it is applied to the measurement data without checking normality of the height distribution. Nevertheless the fractal approach was quite popular for characterization of rough surfaces and their synthesis.

There is a very popular claim that the surface topography shows self-affine fractal-like scaling that is manifested as a power-law  $G(\omega) \propto 1/\omega^{(1+2H)}$ . Here  $H$  is the so-called Hurst exponent. The papers that develop the fractal approach to surface topography often claim that the statistical properties of the topography are invariant under quasi-homogeneous transformation of coordinates (self-affinity in the fractal terminology), i.e. if  $\mathbf{x} \rightarrow \lambda \mathbf{x}$ , then  $z(\mathbf{x}) \rightarrow \lambda^H z(\mathbf{x})$ , where  $z(\mathbf{x})$  is the surface topography height at point  $\mathbf{x}$ ,  $\lambda$  is any positive scaling factor and  $H$  is the so-called self-affine exponent or the Hurst parameter that describes the trend of the topography heights. The arguments that the Hurst parameter (exponent) that follows from the latter definition is the same as the above-mentioned former one (it connects  $H$  with the power-law behaviour of the PSD) are rather vague.

Jeti & Ostoja-Starzewski [34] wrote that the property of self-affinity relates to two key statistical parameters: the  $D$  (which represents the ‘roughness’) and  $H$  (which represents the ‘spatial memory’). They repeated also the common statement about self-affine fractals that the exponent  $H$  is directly related to  $D$  and the Euclidean dimension  $E$ :  $H = E - D$ , where  $E = 2$  for a profile and  $E = 3$  for a surface.

The above claims and similar statements about universality of fractal nature of roughness caused development of various fractal approaches to surface roughness description. In fact (e.g. [35–36]) a very rough surface and a polished surface can have the same  $D$ . [37,38] showed that for the parametric-homogeneous (PH) fractal functions (it is a special class of functions obeying the law of discrete self-similarity), the trend of a function (usually attributed to  $H$ ) and its fractal dimension are not connected to each other. In fact, he showed that PH-functions may have arbitrary prescribed trends keeping the same  $D$ . Using the terminology by Jeti & Ostoja-Starzewski [34], one can say that  $H$  and  $D$  are decoupled. The fractal approaches to surface topography are discussed in detail by Borodich *et al.* [35]. In particular, they argued that the both ‘self-affine fractal’ and ‘Hurst exponent’ terms are ill-defined.

Often the Weierstrass–Mandelbrot (W–M) fractal function is used as synthetic fractal surface for application in tribology. Majumdar & Bhushan [39] suggested to use the following truncated W–M function

$$\tilde{W}(x; p) = \Lambda^{(D-1)} \sum_{n=n_1}^{\infty} p^{(D-2)n} \cos 2\pi p^n x, \quad 1 < D < 2, \quad p > 1, \quad (2.3)$$

for representation of surface roughness. Here  $n_1$  is an integer number, which corresponds to the low cut-off frequency of the profile, and  $\Lambda$  is the so-called characteristic length scale of the profile. The number  $n_1$  depends on the length  $L$  of the sample and is given by  $p^{n_1} = 1/L$  and the parameter  $\Lambda$  determines the position of the spectral density along the power axis. The graph of  $\tilde{W}$  was suggested as a synthetic roughness profile with a power-law fractal behaviour mimicking the fractal dimension of a real surface.

It was often argued that both parameters  $\Lambda$  and  $D$  of the function  $W$  or  $\tilde{W}(x; p)$  are scale-invariant characteristics of the roughness. The W–M function was even considered as a general fractal distribution function for rough surface profiles [40]. However, the non-truncated W–M function is a particular case of PH functions, and it is possible to construct a PH-function having prescribed fractal dimension and arbitrary trend [37,38]. Hence, the W–M function cannot be considered as a general example of fractal roughness. Illustrative examples given in [37,38,41] and [42,43] demonstrated the insufficiency of fractal dimension alone in capturing the contact behaviour of rough surfaces. In addition, Bhushan [44] pointed out that experimental studies revealed non-uniqueness of the parameters  $\Lambda$  and  $D$  in the fractal model, highlighting their dependence on measurement instrumentation and resolution.

Although nowadays the fractal approach is less popular than it was about 20 years ago, the PSD approach is still actively used. However, the fractal and PSD approaches have the same common drawback. If in addition to the profile  $z(x)$  one considers an inverted profile  $y(x)$  defined as  $y(x) = -z(x)$ , then both profiles  $z(x)$  and  $y(x)$  have the same auto-correlation function and power spectrum in both  $(x, z)$  and  $(x, y)$  coordinate systems. If  $z(x)$  has a fractal graph, then, evidently,  $y(x)$  has the same fractal dimension. Thus, neither fractal dimension nor PSD alone can give a full description of surface roughness.

### 3. Representative elementary pattern of roughness

Accurately representing rough surfaces typically necessitates the use of very large datasets capturing surface height information. This creates difficulties in the application of conventional numerical methods, e.g. the Polonsky–Keer method, to rough contact studies impractical. To

achieve a requested numerical accuracy, the grid, on which fast Fourier transform (FFT) is performed, needs to be extended far beyond the contact area, leading to a substantial bottleneck in terms of computational time. However, the computations may be performed using a smaller amount of measurement data, namely FFT can be applied on a smaller interval of the SRPSR or a close pattern. Let us introduce the notion of the representative elementary pattern of roughness mirroring the notion of the representative elementary volume used in mechanics of random inhomogeneous materials. As it has been mentioned, the REPR is the smallest interval (or area) over which a measurement can be made that will yield a value representative of the whole from the statistical point of view. It is impossible to possess a representative property for patterns smaller than the REPR.

### (a) The KS statistic and moving window techniques

The KS statistic (also known as the KS Goodness of Fit test or the KS-test) compares the data of a sample and a given distribution or two samples and allows us to understand if they have the same distribution [45]. If the KS statistic is used to test if the distribution observed on a sample came from a specified theoretical distribution, e.g. the Gaussian distribution, then it is referred to as a one-sample KS-test. Examples of applications of the one-sample KS-test to check whether the surface roughness is normal were given by Borodich *et al.* [29] and Pepelyshev *et al.* [30]. If the KS statistic is used to test whether two samples came from the same distribution, then it is referred to as a two-sample KS-test. The details of applications of the two-sample KS-test to subsamples extracted by moving windows are discussed in this section.

Consider a profile that is a sample of surface roughness measurements and another sample that is a subset of the whole profile. The hypotheses  $H_0$  and  $H_1$  of the KS-test are the following,  $H_0$ : the subset sample has the same population distribution as the whole profile and  $H_1$ : the subset sample does not represent the full population distribution.

Moving window (or rolling window) techniques slide a selection window through the whole sample of measurements for analysis of the roughness data in the window. In such a manner, moving window is used to select a subset sample. Because the total number of measurement points in the sample is fixed the moving window techniques are designed for retrospective application [12,46,47]. Note that during movement of the window from left to right, a new point is added to the subset sample at the right and the left point is removed. In general, the moving window allows us to calculate various local statistical properties of the whole sample within the window. Owing to the assumption that the profile is homogeneous and it contains a sufficient number of asperities for the apparent properties to be independent of the scale of consideration, it is expected that asperities for the REPR-based synthesized profile will be similar to asperities for the whole profile.

### (b) Extraction of the REPR

To resolve the problem formulated by Lubrecht & Venner [8], we need to collect experimental measurements of the surface roughness (5–10 profiles) that may be considered as representative samples of the surface roughness. Let each of the samples have the same length  $N$ , that is, the total number of measurements on each profile is  $N$ . Applying the KS statistic to each pair of these profiles, we can check if all these profiles have the same height distribution. If profiles are not similar to each other, this indicates that the surface is not homogeneous and should be studied by segments. If they are, then the procedure of extraction of the REPR for a surface can be formulated as follows. Create a joint profile by merging these several profiles. If we took  $m$  profiles then the length of the joint profile is equal to  $K = mN$ . To find the pattern, we slide a window of length  $N_s$  along each of the  $m$  profiles and compute a similarity between the subset sample within the window and the joint profile using the KS statistic. Then a REPR is

constructed as a subset sample such that the statistical characteristics of the REPR are the same as the characteristics of the surface.

The algorithm of extraction of the REPR formally is as follows. First, we take the joint roughness profile if  $m > 1$  or the single whole profile, which is a series of heights  $z_1, z_2, \dots, z_K$  where  $K = mN$ . Second, we take the length of the moving window as  $N_s$  where  $N_s < N$  and slide this window along each of the profiles. Specifically, for the starting point  $i$ ,  $0 \leq i \leq N - N_s$ , we select the subset sample  $(z_{j,i+1}; z_{i+2}; \dots; z_{j,i+N_s})$ , which is a series of heights extracted by the sliding window from the  $j$ -th profile. Third, we compute a similarity between the long series  $z_1, z_2, \dots, z_K$  of the joint profile and the subset sample  $(z_{j,i+1}; z_{i+2}; \dots; z_{j,i+N_s})$  within the moving window with the shift  $i$  using the KS statistic

$$D_{K,N_s;j:i} = \sup_x \left| F_{\text{joint},K}(x) - F_{j,N_s}(x) \right|,$$

where  $F_{\text{joint},K}(x)$  and  $F_{j,N_s}(x)$  are the cumulative distribution functions for two samples, respectively. Fourth, for the fixed window length  $N_s$ , we define a subset sample that minimizes the KS statistic with respect to the shift  $i$ . Also, we consider the KS-based distance measure defined by

$$D_K(N_s) = \min_{\substack{j=1,\dots,m \\ i=1,\dots,N-N_s}} D_{K,N_s;j:i} \quad (3.1)$$

as a function  $N_s$ . Finally, choose  $N_s$  such that the measure  $D_K(N_s)$  is close to zero and  $N_s$  is not big.

The chosen value  $N_s$  is the length of the REPR and the corresponding subset sample which yields  $D_K(N_s)$  is the REPR of the surface.

In figure 1, we show a typical behaviour of the KS-based distance measure  $D_K(N_s)$ . We can see that  $D_K(N_s)$  has the decreasing tendency on  $N_s$ . For very small  $N_s$ , the measure  $D_K(N_s)$  is large because a very short segment cannot sufficiently well represent the whole profile. In addition, we have  $D_K(N_s) \approx 0$  for large  $N_s$  because the large segment is similar to the whole profile. We recommend to choose  $N_s$  as the smallest integer such that  $D_K(N_s) < 0.05$ . For example, in figure 1, candidates for  $N_s$  would be just over 50 or around 80. If  $N_s$  also satisfies the constraint  $N_s = 2^b$  for some integer  $b$  then the REPR with  $2^b$  points will be called the FFT-REPR.

## 4. Construction of the SRPSR

Formally, one could use the REPR obtained in a numerical solver for simulation of contact between rough surfaces. However, as one can see in the following figures, usually the height for the last point is not equal to the height for the first point of the REPR. Consequently, the formal employment of the REPR will cause artificial jumps in the synthetic profile and, in turn, the singularities of the stress fields. Hence, the SRPSR must not only be statistically representative of the entire surface but also adhere to additional criteria specific to the chosen contact problem formulation and numerical approach.

Note that any pattern that includes the REPR is also a representative pattern of surface roughness. If the numerical solver does not have any restriction on the number of the points in the SRPSR, then a pattern of the length  $2N_s$  obtained from the REPR by its mirror symmetry can be taken as the SRPSR. Indeed, the heights at the first point and at the last point are the same and, therefore, there are no artificial singularities in the profile.

In fact, the solvers can have restrictions on the number of the points in the profile. Let us consider as an example the Polonsky-Keer numerical scheme. The Polonsky-Keer algorithm combines the use of the FFT and the multi-level multi-summation techniques. This allows to



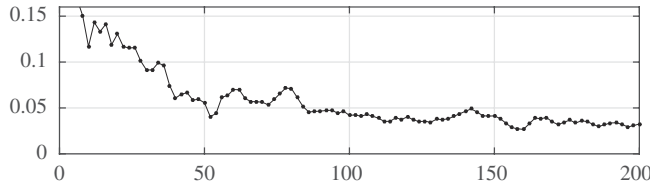


**Figure 1.** The KS-based distance measure  $D_K(N_s)$  as a function of  $N_s$  for a roughness profile of a steel sample obtained by a profilometer,  $K = N = 668$ .

reduce greatly the number of arithmetic operations required by the algorithm [6]. However, the employment of FFT requires that the profile contains  $2^b$  points where  $b$  is some integer. Hence, we will need to extend the length of the pattern and include several additional points that the total length of the pattern will satisfy this condition. For example, if  $N_s = 52$ , then we need to add 12 additional points to extend the profile to a FFT-REPR having  $2^6$  points and then to use the mirror symmetry of the pattern. Hence, the final length of the SRPSR is  $2^7$ .

### (a) Metallic surfaces

Tribological characterization of grinding-induced roughness on engineering surfaces has been performed across nano and micro scales to understand surface features. The heights of the micro-asperities were determined by the stylus profilometer (Taylor Hobson Form Talysurf 2 profilometer), while the data for nano/atomic scale were obtained by the AFM instrument (XE-100 from Park Systems). The resolution scale of the AFM device is 2 nm vertically and 5 nm laterally. The profilometer is fitted with 250 nm in the  $x$  (measurement) direction, 1 micron in the  $y$  direction and 19 nm vertically. Let us study several datasets obtained by these instruments.

In figure 2, one can see a roughness profile of a bronze sample obtained by AFM, where measurements  $z_k$  are taken at points  $x_k = 0.1758k \mu\text{m}$ ,  $k = 1, \dots, K$ ,  $K = 256$ . The REPR of length 104 was extracted. Then it has been extended to the FFT-REPR having 128 points.

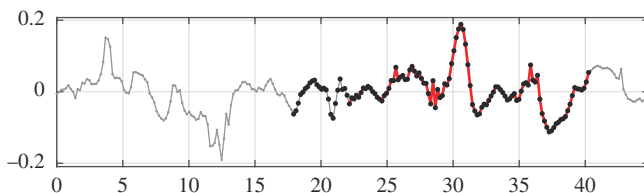
In figure 3, we show the roughness profile of a copper sample obtained by AFM, where measurements  $z_k$  are taken at points  $x_k = 0.15625k \mu\text{m}$ ,  $k = 1, \dots, K$ ,  $K = 256$ , the REPR of length 55 that has been extended to the FFT-REPR having 64 points.

Figure 4 presents the roughness profile obtained by the profilometer on a steel gear surface, where measurements  $z_k$  are taken at points  $x_k = 1.5k \mu\text{m}$ ,  $k = 0, 1, 2, \dots, K$ ,  $K = 667$ ; the REPR of length 53 that have been extended to the FFT-REPR having 64 points.

Comparing profiles in figures 2–4, we see that the REPR for the bronze sample is longer than the REPR for the copper sample and a steel gear surface because short segments of the bronze roughness profile are very different from each other.

### (b) Carbon coating and polydimethylsiloxane

We consider the roughness of two amorphous carbon (a-C) films that were deposited on silicon substrates by a DC-pulsed magnetron sputtering in Ar atmosphere ( $5 \times 10^{-3}$  mbar) using a graphite target at 300 W. The pulse conditions were set at 250 kHz of frequency, 496 ns of duration (87.6% of duty cycle). A negative bias of approximately 150 V was applied to the substrate in one of the cases. Both processes were carried out at room temperature and the measured thicknesses were 700 and 1300 nm for biased and non-biased samples, respectively. Carbon-based coatings prepared by plasma-assisted deposition methods at room temperature are generally amorphous as they are synthesized in conditions out of thermodynamic



**Figure 2.** The REPR (red colour) of length 104 and the FFT-REPR having 128 points (black dots) for a roughness profile of the bronze sample measured by AFM; scale units are  $\mu\text{m}$ .

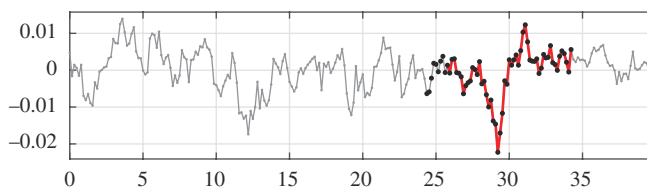


**Figure 3.** The REPR (red colour) of length 55 and the FFT-REPR having 64 points (black dots) for a roughness profile of the copper sample measured by AFM; scale units are  $\mu\text{m}$ .

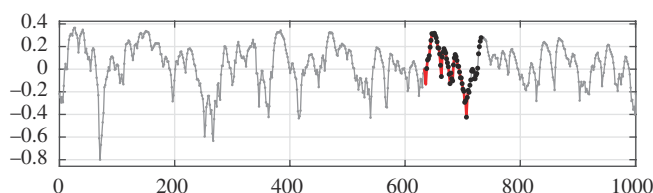


**Figure 4.** The REPR (red colour) of length 53 and the FFT-REPR having 64 points (black dots) for a roughness profile of the steel sample measured by the profilometer; scale units are  $\mu\text{m}$ .

equilibrium. There are many papers based on DLC and a-C coatings where these structural characteristics are proven (e.g. [48]).

Hardness measurements carried out with a MTS Nanoindenter II XP using the continuous stiffness measurement technique and a diamond Berkovich (three-sided pyramid) indenter tip gave 43 (biased) and 14 (non-biased) GPa, respectively. Scanning electron microscopy data were recorded in a FEG Hitachi S4800 microscope operating at 5 kV.

The AFM system used to measure the nanoscale topography of the sample was the XE-100 model from Park Systems. The probes employed were the CSG model from NT-NDT. These probes are utilized for contact mode AFM operations and are designed with a rectangular-type cantilever, which is Au-coated on its reflective side. These probes are made of single-crystal silicon and have a nominal force constant of 0.11 N/m, as stated by the manufacturer. The typical curvature radius of the tip mounted at the free end of the cantilever is stated to be 6 nm. In particular, the dimension of a scanned area was set at  $30\ \mu\text{m} \times 30\ \mu\text{m}$  for the a-C sample. However, the scanned area was  $40\ \mu\text{m} \times 40\ \mu\text{m}$  for the bias a-C sample. In all cases a  $256 \times 256$  grid was used. This means that the AFM step was 117 nm for the area  $30\ \mu\text{m} \times 30\ \mu\text{m}$  and 156 nm for the area  $40\ \mu\text{m} \times 40\ \mu\text{m}$ , respectively.

In figure 5 we show a roughness profile of the a-C sample, the REPR of length 53 and the FFT-REPR having 64 points.

In figure 6, we show a roughness profile of the a-C (bias) sample, the REPR of length 48 and the FFT-REPR having 64 points.

Finally, we consider the roughness of polydimethylsiloxane (PDMS) polymer. This material was used earlier by Purto *et al.* [49] to prepare epoxy resin replicas of surfaces having different

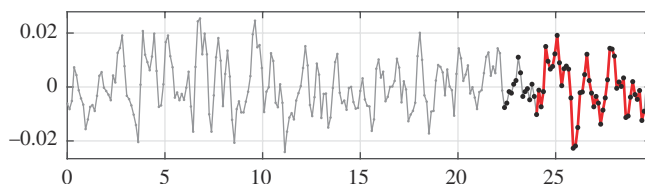


**Figure 5.** The REPR (red colour) of length 53 and the FFT-REPR having 64 points (black dots) for a roughness profile of the a-C sample measured by AFM; scale units are  $\mu\text{m}$ .

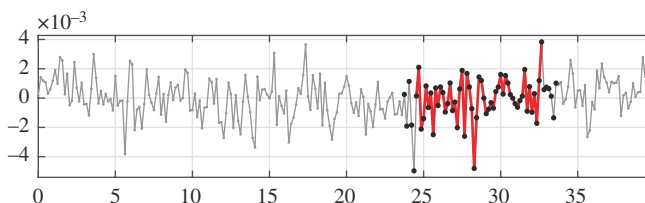


**Figure 6.** The REPR (red colour) of length 48 and the FFT-REPR having 64 points (black dots) for a roughness profile of the a-C (bias) sample measured by AFM; scale units are  $\mu\text{m}$ .

topography and conduct depth-sensing indentation of the samples using a micro-force tester with a spherical smooth probe made of the compliant PDMS polymer in order to compare values of the force of adhesion with the surfaces. In particular, a clean smooth glass surface and polishing papers of nominal asperity size  $0.3\ \mu\text{m}$  were used as templates for preparation of the epoxy resin replicas. The roughness of test surfaces was measured using a white light interferometer (Zygo NewView 6000; Zygo Corporation, Middlefield, CT, USA) at a magnification of 50. As has been mentioned above, the roughness of the samples was tested by Pepelyshev *et al.* [30].

In figure 7, we show the roughness profile of the PDMS polymer, the REPR of length 84 and the FFT-REPR having 128 points.

As can be seen, the SRPSRs obtained for all samples are shorter than the original profiles. If the algorithms for solving the contact problems between rough surfaces do not require their extensions to  $2^b$  points then the appropriate SRPSRs may be extended in other ways.

## 5. Conclusion

It is known that the vast amount of data required for realistic descriptions of rough surfaces renders conventional numerical methods in contact mechanics computationally prohibitive. There were developed various effective numerical solvers for simulations of contact between rough surfaces, e.g. the Polonsky-Keer solver based on employment of FFT [6]. However, to achieve a requested numerical accuracy, the grid, on which FFT is performed, needs to be extended far beyond the contact area, leading to an essential growth of the computation time. A fundamentally new approach to problems related to the synthesis of rough surfaces of solids has been presented. The approach is based on introduction of a new concept, the representative elementary pattern of roughness that is the smallest interval (or area) over which a measurement can be made that represents statistically the whole surface. The idea of the REPR term is similar to the idea of the representative elementary volume used in mechanics of random inhomogeneous materials [50].

It has been shown that statistical time-series analysis methods, such as the moving window technique, have proven effective in extracting the REPR from experimental data. The two-sample KS-test (the KS statistic) has been used to compare the distribution of the sample within

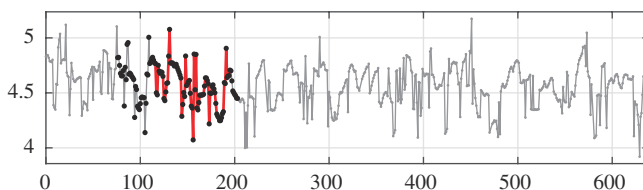


**Figure 7.** The REPR (red colour) of length 84 and the FFT-REPR having 128 points (black dots) for a roughness profile of the PDMS polymer sample with nominal roughness 0.3 measured by white light interferometry; scale units are  $\mu\text{m}$ .

the moving window and the distribution of the whole sample. Hence, statistically, the REPR replicates the original rough surface, capturing its essential characteristics for analysis.

Usually, the synthesized surface cannot be viewed as a union of several copies of the REPR. Indeed, a series of REPRs will produce jumps at the joints of two REPRs that, in turn, cause singularities in stress fields of contacting solids. Hence, there is a need to find such a size of the moving window and its location that the appropriate pattern satisfies not only the condition that it is entirely typical of the whole surface but also satisfies some additional conditions depending on the contact problem formulation and the numerical scheme used. This was the reason for the introduction of another new concept, which is the SRPSR.

Extraction of REPRs of surfaces and constructions of appropriate SRPSRs are demonstrated on experimental data obtained at micro and atomic/nano scales for several metallic surfaces, amorphous carbon and polymer samples. We argue that surfaces synthesized using our approach cannot be distinguished from the original rough surface and they are convenient for the use of numerical algorithms based on employment of FFT techniques.

**Data accessibility.** The supplementary material contains data and MATLAB code with extraction of the REPR and the FFT-REPR [51].

**Declaration of AI use.** We have not used AI-assisted technologies in creating this article.

**Authors' contributions.** F.M.B.: conceptualization, investigation, methodology, writing—original draft; A.P.: conceptualization, investigation, methodology, visualization, writing—review and editing.

Both authors gave final approval for publication and agreed to be held accountable for the work performed therein.

**Conflict of interest declaration.** The authors declare that they have no competing interests.

**Funding.** No funding has been received for this article.

**Acknowledgements.** The authors are grateful to Professor A. Zhigljavsky (Cardiff University, UK) for his interest in the topic of the research and participation in fruitful discussions, and Professor E. Brousseau (Cardiff University, UK) and Dr. J. C. Sanchez Lopez (Instituto de Ciencia de Materiales de Sevilla, Spain) for their help in acquisition of the experimental data.

## References

1. Whitehouse DJ. 2010 *Handbook of surface and nanometrology*. Boca Raton, FL: CRC Press.
2. Khusu AP, Vitenberg Y, Palmov VA. 1975 *Roughness of surfaces: theoretical probabilistic approach*. Moscow (Russian): Nauka.
3. Greenwood JA. 1992 Problems with surface roughness. In *Fundamentals of friction* (eds IL Singer, HM Pollock), pp. 57–76. Boston, MA: Kluwer. (doi:10.1007/978-94-011-2811-7\_4)
4. Grigoriev AY. 2016 *Physics and microgeometry of technical surfaces*. Minsk (Russian): Belaruskaya Navuka.
5. Polonsky IA, Keer LM. 1999 A numerical method for solving rough contact problems based on the multi-level multi-summation and conjugate gradient techniques. *Wear* **231**, 206–219. (doi:10.1016/S0043-1648(99)00113-1)
6. Polonsky IA, Keer LM. 2000 Fast methods for solving rough contact problems: a comparative study. *J. Tribol.* **122**, 36–41. (doi:10.1115/1.555326)

7. Bora CK, Plesha ME, Carpick RW. 2013 A numerical contact model based on real surface topography. *Tribol. Lett.* **50**, 331–347. (doi:10.1007/s11249-013-0128-8)
8. Lubrecht AA, Venner CH. 1999 Elastohydrodynamic lubrication of rough surfaces. *Proc. Inst. Mech. Eng. Part J J. Eng. Tribol.* **213**, 397–404. (doi:10.1243/1350650991542767)
9. Glover PWJ, Matsuki K, Hikima R, Hayashi K. 1998 Synthetic rough fractures in rocks. *J. Geophys. Res. Sol. Earth* **103**, 9609–9620. (doi:10.1029/97JB02836)
10. Borodich FM, Bianchi D. 2013 Surface synthesis based on surface statistics. In *Encyclopedia of tribology* (eds QJ Wang, YW Chung), pp. 3472–3478, vol. 2. New York, NY: Springer. (doi:10.1007/978-0-387-92897-5\_309)
11. Nowicki B. 1985 Multiparameter representation of surface roughness. *Wear* **102**, 161–176. (doi:10.1016/0043-1648(85)90216-9)
12. Golyandina N, Zhigljavsky A. 2020 *Singular spectrum analysis for time series*. Berlin, Heidelberg, Germany: Springer.
13. Abbott EJ, Firestone FA. 1933 Specifying surface quality: a method based on accurate measurement and comparison. *Mech. Eng.* **55**, 569.
14. Borodich FM, Galanov BA, Perepelkin NV, Prikazchikov DA. 2019 Adhesive contact problems for a thin elastic layer: asymptotic analysis and the JKR theory. *Math. Mech. Solids*. **24**, 1405–1424. (doi:10.1177/1081286518797378)
15. Zhuravlev VA. 1940 On question of theoretical justification of the Amontons-Coulomb law for friction of unlubricated surfaces. *J. Tech. Phys.* **10**, 1447–1452.
16. Greenwood JA, Williamson JBP. 1966 Contact of nominally flat surfaces. *Proc. R. Soc. Lond. A* **295**, 300–319. (doi:10.1098/rspa.1966.0242)
17. Whitehouse DJ, Archard J.F. 1970 The properties of random surfaces of significance in their contact. *Proc. R. Soc. Lond. A*. **316**, 97–121. (doi:10.1098/rspa.1970.0068)
18. Whitehouse DJ. 1982 The parameter rash — is there a cure? *Wear* **83**, 75–78. (doi:10.1016/0043-1648(82)90341-6)
19. BS-EN-ISO-4287:2000. 2009 *Geometrical product specification (GPS) -surface texture: profile method - terms, definitions and surface texture parameters. EN ISO 4287:1998+A1:2009*.
20. ASME B46.1-2002. 2002 *Surface texture (surface roughness, waviness and lay)*. An American National Standard. ASME.
21. Borodich FM. 2013 Fractal contact mechanics. In *Encyclopedia of tribology* (eds QJ; Wang,, YW Chung), pp. 1249–1258, vol. 2. Boston, MA: Springer. (doi:10.1007/978-0-387-92897-5\_512)
22. Linnik Y, Khusu AP. 1954 Mathematical and statistical description of unevenness of surface profile at grinding. *Uspekhi. Mat. Nauk.* **9**, 255.
23. Linnik Y, Khusu AP. 1954 Mathematical and statistical description of unevenness of surface profile at grinding. *USSR Acad. Sci. Div. Techn. Sci.* **20**, 154–159.
24. Maugis D. 2000 *Contact, adhesion and rupture of elastic solids*. Berlin, Germany: Springer-Verlag.
25. Nayak PR. 1971 Random process model of rough surfaces. *J. Lubr. Technol.* **93**, 398–407. (doi:10.1115/1.3451608)
26. Nayak PR. 1973 Some aspects of surface roughness measurement. *Wear* **26**, 165–174. (doi:10.1016/0043-1648(73)90132-4)
27. Bibby B.M, Michael Skovgaard I, Sørensen M. 2005 Diffusion-type models with given marginal distribution and autocorrelation function. *Bernoulli* **11**, 191. (doi:10.3150/bj/1116340291)
28. Thode HC. 2002 *Testing for normality*. New York, NY: Marcel Dekker.
29. Borodich FM, Pepelyshev A, Savencu O. 2016 Statistical approaches to description of rough engineering surfaces at nano and microscales. *Tribol. Int.* **103**, 197–207. (doi:10.1016/j.triboint.2016.06.043)
30. Pepelyshev A, Borodich FM, Galanov BA, Gorb EV, Gorb SN. Adhesion of soft materials to rough surfaces: experimental studies, statistical analysis and modelling. *Coatings* **8**, 350. (doi:10.3390/coatings8100350)
31. Borodich FM, Brousseau E, Clarke A, Pepelyshev A, Sánchez-López JC. 2019 Roughness of deposited carbon-based coatings and its statistical characteristics at nano and microscales. *Front. Mech. Eng.* **5**, 73. (doi:10.3389/fmech.2019.00024)

32. Sayles RS, Thomas TR. 1978 Surface topography as a nonstationary random process. *Nature* **271**, 431–434. (doi:10.1038/271431a0)
33. Berry MV, Hannay JH. 1978 Topography of random surfaces. *Nat. New Biol.* **273**, 573. (doi:10.1038/273573a0)
34. Jetti YS, Ostoja-Starzewski M. 2022 Elastic contact of random surfaces with fractal and Hurst effects. *Proc. R. Soc. A.* **478**. (doi:10.1098/rspa.2022.0384)
35. Borodich FM, Jin X, Pepelyshev A. Probabilistic, fractal, and related techniques for analysis of engineering surfaces. *Front. Mech. Eng.* **6**. (doi:10.3389/fmech.2020.00064)
36. Borodich FM, Pepelyshev A, Jin X. 2024 A multiscale statistical analysis of rough surfaces and applications to tribology. *Mathematics* **12**, 1804. (doi:10.3390/math12121804)
37. Borodich FM. 1998a Parametric homogeneity and non-classical self-similarity. i. Mathematical background. *Acta Mech.* **131**, 27–45. (doi:10.1007/BF01178243)
38. Borodich FM. 1998b Parametric homogeneity and non-classical self-similarity. ii. Some applications. *Acta Mech.* **131**, 47–67. (doi:10.1007/BF01178244)
39. Majumdar A, Bhushan B. 1990 Role of fractal geometry in roughness characterization and contact mechanics of surfaces. *Trans. ASME J. Tribol.* **112**, 205–216. (doi:10.1115/1.2920243)
40. Blackmore D, Zhou JG. 1996 A general fractal distribution function for rough surface profiles. *SIAM J. Appl. Math.* **56**, 1694–1719. (doi:10.1137/S0036139995283122)
41. Borodich FM. 1993 Similarity properties of discrete contact between a fractal punch and an elastic medium. *Cr. Ac. Sc. (Paris), Ser. 2* **316**, 281–286.
42. Borodich FM, Onishchenko DA. 1993 Fractal roughness for problem of contact and friction (the simplest models). *J. Frict. Wear.* **14**, 452–459.
43. Borodich FM, Onishchenko DA. 1999 Similarity and fractality in the modelling of roughness by a multilevel profile with hierarchical structure. *Int. J. Solids Struct.* **36**, 2585–2612. (doi:10.1016/S0020-7683(98)00116-4)
44. Bhushan B. 1995 Fractal theory of the temperature distribution at elastic contacts of fast sliding surfaces - discussion. *J. Tribol.* **117**, 214. (doi:10.1115/1.2831228)
45. Conover WJ. 1999 *Practical nonparametric statistics*. New York, NY: John Wiley and Sons.
46. Bower T. 2022 *Introduction to computational engineering with MATLAB*. Abingdon, UK: Chapman and Hall/CRC.
47. Schelter B, Winterhalder M, Timmer J. 2006 *Handbook of time series analysis*. Weinheim, Germany: Wiley-VCH.
48. Lin J, Moore JJ, Sproul WD, Mishra B, Wu Z, Wang J. 2010 The structure and properties of chromium nitride coatings deposited using dc, pulsed dc and modulated pulse power magnetron sputtering. *Surf. Coatings Technol.* **204**, 2230–2239. (doi:10.1016/j.surfcoat.2009.12.013)
49. Purtov J, Gorb EV, Steinhart M, Gorb SN. 2013 Measuring of the hardly measurable: adhesion properties of anti-adhesive surfaces. *Appl. Phys.* **111**, 183–189. (doi:10.1007/s00339-012-7520-3)
50. Willis JR. 1981 Variational and related methods for the overall properties of composites. *Adv. Appl. Mech.* **21**, 1–78. (doi:10.1016/S0065-2156(08)70330-2)
51. Borodich FM, Pepelyshev A. 2024 Data from: Synthesis of engineering surfaces using representative elementary patterns of roughness. Figshare. (doi:10.6084/m9.figshare.c.7441730)